THE JOURNAL OF PHYSICAL CHEMISTRY B

ARTICLE

pubs.acs.org/JPCB

Comprehensive Study of Tartrazine/Cationic Surfactant Interaction

Afshin Asadzadeh Shahir,[†] Soheila Javadian,*[,†] Bi Bi Marzieh Razavizadeh,[‡] and Hussein Gharibi[†]

[†]Department of Physical Chemistry, Tarbiat Modares University, P.O. Box 14115-117, Tehran, Iran

[‡]Khorasan Research Institute for Food Science & Technology, 12th km of Mashhad-Quchan Highway, P.O. Box 91735-139, Mashhad, Iran

Supporting Information

ABSTRACT: Interaction of a food dye, tartrazine, with some cationic conventional and gemini surfactants, tetradecyltrimethylammonium bromide (TTAB), *N*,*N*′-ditetradecyl-*N*,*N*,*N*′,*N*′-tetramethyl-*N*,*N*′-butanediyl-diammonium dibromide (14,4,14), and *N*,*N*′-didodecyl-*N*,*N*,*N*′,*N*′-tetramethyl-*N*,*N*′-butanediyl-diammonium dibromide (12,4,12), were first investigated comprehensively employing conductometry, tensiometry, and UV−visible spectroscopy. Tartrazine was found to behave in the same manner as aromatic counterions. The formation of ion pairs reflected as a considerable increase of the surfactant efficiency in tensiometry plots and their stoichiometry were determined by Job's method of continuous variations. For the tartrazine/TTAB system, nonionic DS_3, ionic DS^{2-}, and/or DS_2^- ion pairs, their small premicelles, and tartrazine-rich micelles were constituted as well as dye-containing TTAB-rich micelles. Insoluble J-aggregates of DS^- ion pairs and cylindrical surfactant-rich micelles were also formed in tartrazine/gemini surfactant systems and recognized by transmission electron microscopy. The zeta potential and the size of the aggregates were determined using dynamic light scattering and confirmed the suggested models for the processes happening in each system. Cyclic voltammetry was applied successfully to track all of these species using tartrazine's own reduction peak current for the first time.

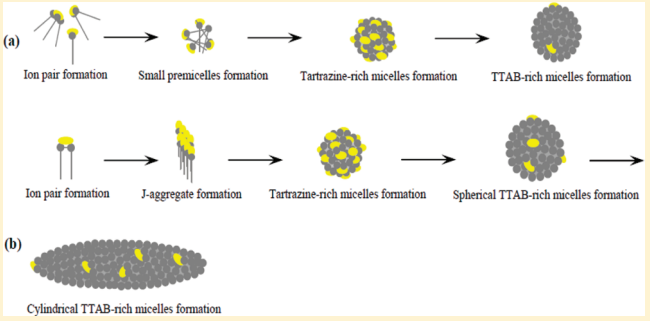

1. INTRODUCTION

Dye/surfactant mixtures have become the subject of recent research in chemistry, textiles, pharmacology, biochemistry, and biology. The application of surfactants as dye solubilizing, dispersing, leveling, and wetting agents in most textile processes[1] and cosmetic products[2] have recently interested many researchers in the field of dye/surfactant interactions. These researchers are also investigating the development of new analytical methods for the determination of dyes, surfactants, and drugs;[3−5] the removal of environmentally hazardous dyes from industrial effluents using surfactants;[6,7] and the formation of various dye-surfactant aggregates important in photophysics[8,9] and that serve as suitable models for biological research.[10]

Although different combinations of various types of dyes and surfactants have been studied thus far, the contribution of both electrostatic and hydrophobic forces to dye/surfactant interactions and to the analogous interactions in biological processes needs to be determined; thus, this has driven the study of the interactions in oppositely charged dye/surfactant systems. Depending on the structure and concentration of both components, these systems involve the formation of various species such as dye/surfactant complexes and salts, ion pairs and their aggregates, self-aggregates of dye, dye-rich premicelles, and pure micelles of surfactants with solubilized dye monomers. These species have been detected successfully during the study of dye/surfactant systems by a wide variety of techniques such as conductometry,[11−13] tensiometry,[14−16] UV−vis spectroscopy,[17−19] fluorescence spectroscopy,[20,21] potentiometry,[22] and polarography.[23] Although cyclic voltammetry has been widely used to investigate surfactant systems,[24,25] to date, there is no report on the application of cyclic voltammetry to study dye/surfactant mixtures. The addition of even small amounts of electroactive probes like (2,2,6,6-tetramethylpiperidin-1-yl)oxyl or (2,2,6,6-tetramethylpiperidin-1-yl)oxidanyl (TEMPO) and ferrocene to dye/surfactant solutions can cause noticeable changes and errors in the behavior of the system. Therefore, the possibility for the application of cyclic voltammetry to investigate dye/surfactant systems hinges on the components' own electroactive properties.

In the present work, the efficiency of cyclic voltammetry in the qualitative identification of various dye/surfactant aggregates and probable phase changes has been studied for the first time using the electroactive dye, tartrazine, in addition to cationic conventional and gemini surfactants. Tartrazine (FD and C Yellow No. 5) is a synthetic monoazo pyrazolone dye with three negative charges (Figure 1) and has a widespread use in foodstuffs, cosmetics, textiles, and pharmaceutical products as a colorant. The azo group of tartrazine can undergo a well-defined, two-step, two-electron reduction that is reversible in acidic pH ranges and

Received: June 1, 2011
Revised: October 1, 2011
Published: October 03, 2011

ACS Publications © 2011 American Chemical Society

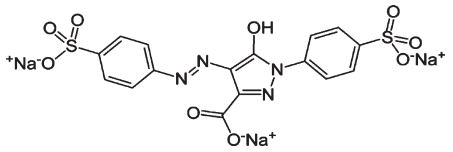

Figure 1. Molecular structure of tartrazine (M.W. = 534.36 g/mol).

becomes quasi-reversible in a neutral medium.[26] Much research has dealt with tartrazine's biological effects[27] and its removal from industrial effluents[28] because it has been associated with some health problems such as hyperactivity, asthma, itching, migraines, and cancer. There are, nevertheless, very few reports on the investigation of its interaction with surfactants.[29]

Here, the interaction of tartrazine with conventional and gemini cationic surfactants has been studied comprehensively using conductometry, tensiometry, UV−visible spectroscopy, zeta potential measurements, dynamic light scattering (DLS), and transmission electron microscopy (TEM) techniques. Cyclic voltammetry has been used efficiently in investigating dye/surfactant interactions, and the precise knowledge of the system's behavior has allowed qualitative monitoring of the variation in the tartrazine reduction peak current in the presence of various surfactant concentrations.

2. EXPERIMENTAL SECTION

2.1. Materials. Tetradecyltrimethylammonium bromide (TTAB), 99% pure, and potassium chloride (KCl) were purchased from Aldrich and Merck, respectively. Commercial tartrazine (Saujanya Co., Pakistan), *N*,*N*′-ditetradecyl-*N*,*N*,*N*′,*N*′-tetramethyl-*N*,*N*′-butanediyl-diammonium dibromide (14,4,14), and *N*,*N*′-didodecyl-*N*,*N*,*N*′,*N*′-tetramethyl-*N*,*N*′-butanediyl-diammonium dibromide (12,4,12) were gifts from Dr. Tehrani-Bagha of the Institute for Colorants, Paints and Coatings, Tehran, Iran. Whole solutions were prepared using double distilled water. Solution pHs were in the range of 6.5 to 6.7, so no buffer was used. For all of the experiments, solutions with a constant concentration of tartrazine (0.02 mM) and various concentrations of surfactants were prepared, and the temperature was maintained constant at 25 ± 0.1 °C by circulating thermostatted water through the jacket of the solution vessel.

2.1. Methods. *2.2.1. Specific Conductivity Measurements.* Conductometric titrations were done using a JENWAY 4510 conductometer. After any injection, the solution was stirred and allowed to equilibrate for 10 min, and then three successive measurements of specific conductivity were performed. The concentration of tartrazine was held constant at 0.02 mM during the titrations. The uncertainty of the measurements was ±0.01 μS/cm.

2.2.2. Surface Tension Measurements. Surface tension measurements were made with a KRÜSS K12 tensiometer, employing the Du-Noüy ring method under atmospheric pressure. First, the glass container was rinsed sequentially until the surface tension of distilled water was measured up to 70−72 mN/m. The platinum ring was thoroughly cleaned by acetone and distilled water, and flamed until glowing temperature before each measurement. Here again, the solution was stirred and allowed to equilibrate for 10 min after any injection of concentrated solution. The concentration of tartrazine was maintained constant at 0.02 mM during the titrations. In all cases, more than three successive measurements were carried out, and the standard deviation did not exceed 0.05 mN/m. The uncertainty of the measurements was ±0.1 mN/m.

2.2.3. UV−Vis Spectroscopy. Tartrazine solutions with the desired concentration of surfactants were prepared and left to equilibrate for 10 min, and then visible absorption spectra were recorded using a SHIMADZU 2100 UV−visible spectrophotometer with a matched pair of glass cuvettes, 1 cm in optical path length. Equimolar solutions (0.02 mM) of tartrazine and gemini surfactants were mixed in various volume fractions to obtain Job's plots.

2.2.4. TEM, DLS, and Zeta Potential Measurements. Zetasizer Nano (Malvern, MRK825-02, UK) was used for DLS and zeta potential measurements. Solutions were prepared and rendered to the operator. The refraction index and viscosity of the solutions were measured at 1.33 and 0.8872 cP, respectively. TEM images were captured using a Philips CM 120 electron microscope operating at 120 kV. Samples were placed on carbon-coated grids and kept waiting for the solvent to vaporize, and then micrographs were obtained.

2.2.5. CV Measurements. Tartrazine/surfactant solutions, containing 0.1 M KCl (as the supporting electrolyte for CV measurements), were prepared. The SAMA 500 electroanalyzer system was employed for this technique. A three-electrode system composed of a platinum disk electrode (0.0314 cm^2) as the working electrode, a platinum foil (2 cm^2) as the counter electrode, and a saturated Ag/AgCl electrode as the reference electrode was used for CV measurements. The working electrode was polished, cleaned by a 1:1 mixture of nitric and sulfuric acids, and then rinsed by distilled water before recording each voltammogram. Electrodes were plunged in solutions for 10 min, and then voltammograms were recorded for each solution with a scan rate of 100 mV/s, and the fifth cycles were saved.

3. RESULTS AND DISCUSSION

3. 1. Self-Aggregation Behavior of Tartrazine Molecules. Some dye molecules are known to form dimers, trimers, or higher aggregates in aqueous solution.[30−33] This self-aggregation process can change the physical properties of the dye solution and cause misunderstandings in the study of dye/surfactant systems. Thus, the self-aggregation of tartrazine molecules was first studied by investigating the validity of the Beer−Lambert law in the concentration range of 0.01 mM to 0.06 mM. As expected, the linearity of absorbance versus concentration (plots are provided as Supporting Information) confirmed the lack of such self-aggregation processes for tartrazine. This effect is likely caused by the intense electrostatic repulsion originating from the negative charges on the molecules. Therefore, a constant concentration of 0.02 mM was chosen for the tartrazine solutions.

3. 2. Formation of Dye/Surfactant Ion Pairs and Their Surface Activity. The formation of any surface active species between oppositely charged dyes and surfactants in bulk solution can also affect the structure of the surface monolayer, giving rise to some obvious changes in the solution surface tension. The presence of tartrazine increased the tendency of TTAB molecules to migrate to the solution surface, and the surface tension began to decrease at much lower TTAB concentrations, leading to faster saturation of the solution surface (Figure 2a). This behavior is common for oppositely charged dye/surfactant systems and is attributed to the formation and adsorption of more hydrophobic dye/surfactant ion pairs.[14] In region I, through the addition of small amounts of TTAB to the tartrazine

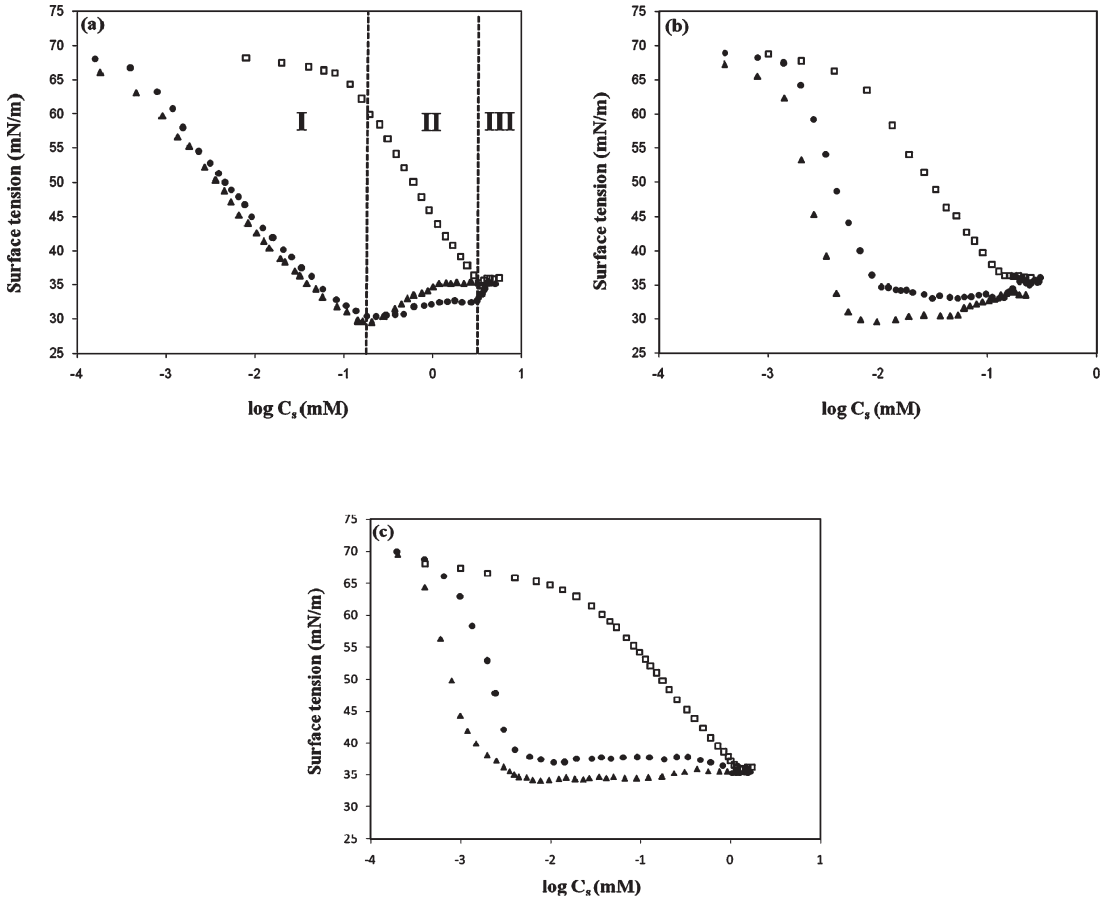

Figure 2. Tensiometry plots for (a) TTAB, (b) 14,4,14, and (c) 12,4,12 in the absence of tartrazine and KCl (□), in the presence of 0.02 mM tartrazine (●), and in the presence of 0.02 mM tartrazine + 0.1 M KCl (▲) at 25 ± 0.1 °C.

solution, some hydrophobic surface active ion pairs are formed. These ion pairs migrate to the surface to form an ion pair-rich monolayer rather than the pure TTAB monolayer that is formed in the absence of tartrazine. Because the addition of an electrolyte to the mixture has no considerable effect on the solution surface tension in this region, it is conceivable that the ion pairs composing the surface monolayer are uncharged. In other words, tartrazine and TTAB can form uncharged DS_3 ion pairs, which behave like nonionic surfactants. As the concentration of TTAB reaches 0.18 mM, the surface is saturated by these ion pairs, and the plot becomes level. This point was deemed C_1. At higher concentrations (region II), a slight increase in the surface tension is observed (2 mN/m) that becomes clearer in the presence of an electrolyte (4 mN/m). This result implies the formation of ion pair aggregates in solution as the appearance of a new phase can provide a medium for monolayer ion pairs to participate in. The aggregation of dye/surfactant ion pairs to form dye-rich micelles following surface saturation has been previously observed in similar systems.[15,16] The sensitivity of the surface tension to the electrolyte in this region shows that the formed ion pairs and their resulting aggregates are probably charged. We hypothesize that the DS_3 ion pairs are highly unstable in the aqueous medium; thus, the components tend to form more hydrophilic, stable DS^{2-}, and DS_2^- instead of DS_3 ion pairs after surface saturation. When the concentration of TTAB nears its critical micelle concentration (CMC) at 3.42 mM (this point was deemed C_2), the surface tension again starts to increase by 4 mN/m and becomes equal to that of the pure TTAB solution (region III). Here again, a likely micellar phase change from tartrazine-rich to TTAB-rich micelles persuades the surface monolayer ion pairs to migrate into these new mediums so that their replacement by pure TTAB molecules increases the solution surface tension. Pure surfactant molecules often have a different (smaller or larger) effectiveness (a measure of the maximum surface tension reduction made by a surfactant) than their resulting ion pairs.

These phenomena were also observed for the gemini surfactants with some partial differences (Figure 2b,c). The formation of tartrazine/gemini surfactant ion pairs and a micellar phase change from tartrazine-rich micelles to surfactant-rich ones were similarly reflected in the tensiometry plots. Here, the solution gradually becomes turbid in region II soon after the surface is saturated by ion pairs and becomes clear again by increasing the gemini surfactant concentration. The turbidity is stable up to 80 °C and for several days. Meanwhile, needle-shaped yellow crystals are formed and grow with time to eventually yield a clear colorless solution phase. Furthermore, the presence of an electrolyte decreases the solution surface tension in region I, unlike the tartrazine/TTAB system, which indicates a charged nature of tartrazine/gemini surfactant ion pairs adsorbed on the surface. To confirm this hypothesis, the stoichiometric ratios of tartrazine and surfactants in their resulting ion pairs were determined using Job's method of continuous variations because this method has been employed previously for some dye/surfactant systems.[34,35]

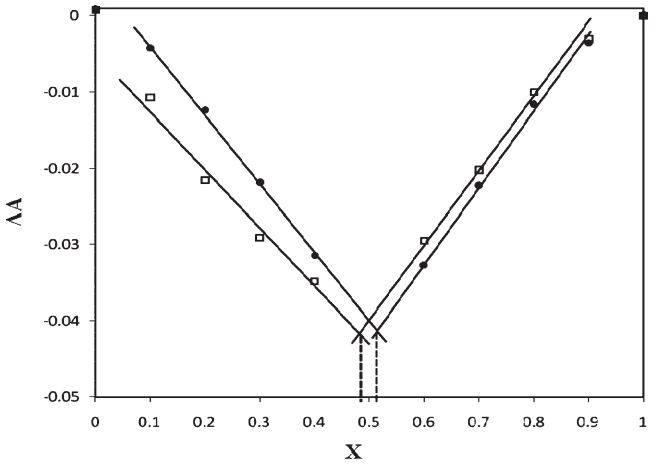

Figure 3. Job's plots for tartrazine/12,4,12 (□) and tartrazine/14,4,14 (●) mixtures.

To obtain Job's plot, various volume fractions of equimolar solutions of dye and surfactant were mixed, and the corrected absorbances of these mixtures (ΔA) were plotted versus the volume fraction of the surfactant solution (X). According to the Beer−Lambert law, if the dye and surfactant do not interact, the total absorbance of the mixture (A_{theo}) is equal to the sum of their individual absorbances as follows:

$$A_{theo} = \varepsilon_S C_S^0 X_S + \varepsilon_D C_D^0 (1 - X_S) \quad (1)$$

where ε_S and ε_D are the molar extinction coefficients of the surfactant and dye, respectively. C_S^0 and C_D^0 are the concentrations of the stock solutions of the surfactant and dye, which are equal ($C_S^0 = C_D^0$). The formation of D_mS_n complexes makes the absorbance of the solution satisfy the following relationship:

$$A_{exp} = \varepsilon_S C_S + \varepsilon_D C_D + \varepsilon_{D_mS_n} C_{D_mS_n} \quad (2)$$

where $\varepsilon_{D_mS_n}$ is the molar extinction coefficient of the complex, and C_S, C_D, and $C_{D_mS_n}$ are the concentrations of the species in the mixture. By calculating A_{theo} and measuring A_{exp}, the corrected absorbances can be obtained for all the mixtures and plotted versus X as follows:

$$\Delta A = A_{exp} - A_{theo} \quad (3)$$

The minimum or maximum of this plot corresponds to the stoichiometric ratio of the dye and surfactant involved in the ion pairs.

As a reminder, this method is applicable only for the systems whose components form only one complex. As expected from the tensiometry plot, more than one species is probably formed for the tartrazine/TTAB system (DS_3, DS^{2-}, and DS_2^-) because no plot was obtained with an obvious minimum or maximum. Conversely, the minimum for gemini surfactants occurs at approximately $X = 0.5$ (Figure 3), which implies a 1:1 stoichiometric ratio. In other words, for the tartrazine/gemini surfactant systems, negatively charged DS^- ion pairs are formed and create a charged surface monolayer whose packing is dependent on the electrolyte concentration.

The surface activity of the surfactants in the absence and presence of tartrazine and an electrolyte were investigated using fundamental data extracted from the tensiometry plots. Their efficiencies have been shown by pC_{20}, which is the negative logarithm of the surfactant concentration needed to reduce the surface tension of the solution by 20 mN/m (C_{20}). The corresponding surface excess concentrations have been calculated using the Gibbs adsorption equation as follows:[36]

$$\Gamma_{max} = \frac{-1}{2.303nRT}\left[\frac{d\gamma}{d \log C}\right]_{T,P} \quad (4)$$

where R and T are the gas constant and temperature, respectively; n is the number of species formed in the solution by the dissociation of the surfactant molecules and is equal to 2 for conventional surfactants and 3 for gemini surfactants. $[(d\gamma)/(d \log C)]$ is the slope of the surface tension plot at the CMC or C_1 point. Using the Γ_{max}, which is the minimum area per surfactant molecule, A_{min} has also been obtained using the following relationship:

$$A_{min} = \frac{10^{18}}{N_A \Gamma_{max}} \quad (5)$$

where N_A is Avogadro's number. The calculated values are shown in Table 1. The presence of tartrazine has a considerable increase in the efficiency of whole surfactants because of the ion pair formation. For gemini surfactants, pure 14,4,14 molecules are more efficient than 12,4,12 molecules; however, the 14,4,14 ion pairs become less efficient than those of 12,4,12. According to previous work, in some dye/surfactant systems where the components interact both hydrophobically and electrostatically, as the hydrophobicity of components increases, the hydrophobic interactions become stronger. Subsequently, ion pair formation is facilitated to give rise to an increase in the ion pair concentration and efficiency and faster surface saturation.[14,15,22] This observation is no longer valid for the tartrazine/gemini surfactant systems described herein because the pC_{20} of the tartrazine/12,4,12 ion pairs is larger than that of the tartrazine/14,4,14 ion pairs. Considering the intense electrostatic attraction between the three negative charges of tartrazine and the two positive charges of the gemini surfactants, we propose that their interaction is mainly electrostatic in nature. Hydrophobic interactions also make a small contribution, whereby the increase in the surfactant chain length makes ion pair formation harder rather than facilitating the resulting ion pairs with longer hydrophobic chains, which are more unstable in aqueous medium. Therefore, at a certain surfactant concentration, many more ion pairs are formed for 12,4,12, and the solution surface is saturated faster in the presence of tartrazine compared to that in 14,4,14. Moreover, the addition of an electrolyte also increases the efficiency of the ionic tartrazine/gemini surfactant ion pairs but not that of the nonionic tartrazine/TTAB ion pairs.

Table 1. Extracted Data from Tensiometry Plots at 25 ± 0.1 °C

	TTAB			12,4,12			14,4,14		
parameter	A[a]	B[b]	C[c]	A	B	C	A	B	C
pC_{20} (mM)	0.24	2.31	2.33	0.8	2.69	3.11	1.54	2.39	2.62
$\Gamma_{max} \times 10^6$ (mol/m^2)	1.81	1.35	1.33	1.13	2.43	3.21	1.32	2.69	3.53
A_{min} (Å^2)	91.7	123	124.8	147	68.3	51.9	125.4	61.7	47.1

[a] In the absence of the tartrazine and electrolyte. [b] In the presence of 0.02 mM tartrazine. [c] In the presence of 0.02 mM tartrazine + 0.1 M KCl.

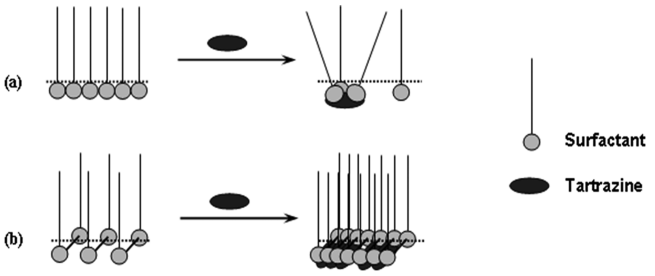

Figure 4. Structure of the surface monolayer made of (a) tartrazine/TTAB ion pairs and (b) tartrazine/gemini surfactant ion pairs.

The excess surface concentration of TTAB has also been decreased by ion pair formation. The nonionic DS_3 ion pairs may spread their three hydrophobic chains over the surface to occupy a larger area and not allow the addition of other ion pairs and monomeric TTAB molecules. For gemini surfactants, the transformation of doubly charged pure gemini surfactant molecules to corresponding DS^- ion pairs with only one charge reduces the electrostatic repulsion between the charged portions. Additionally, the probable electrostatic attraction is generated between the negatively charged ion pairs and the positively charged pure geminis, which results in better packing of the surface monolayer and a considerable increase in Γ_{max} (Figure 4).

3. 3. Aggregation Behavior of Dye/Surfactant Ion Pairs and Micelle Formation in the Bulk Solution. The association of dyes and surfactants in bulk solution can exert various changes such as the appearance of a new band, the shift of the maximum absorption wavelength (λ_{max}), band broadening, and absorption intensity loss in the UV−visible spectrum of dyes. The variation in the maximum absorption wavelength for tartrazine at 426.5 nm with varying surfactant concentration is shown in Figure 5, and the spectra have been attached as Supporting Information. For the tartrazine/TTAB system, a change in λ_{max} was not observed for surfactant concentrations up to 0.49 mM. As discussed above, the solution surface is saturated by tartrazine/TTAB ion pairs at 0.18 mM. Thus, neither ion pair formation nor preliminary small premicelle formation can affect the tartrazine spectrum. However, as the concentration of TTAB reaches 0.49 mM, a slight red shift of 7 nm occurs until the concentration reaches 3.61 mM at the C_2 point where the λ_{max} becomes constant at approximately 435 nm. According to our knowledge of the system from tensiometry, there is a phase change from previously formed tartrazine-rich micelles to TTAB-rich ones at this C_2 point, so it is logical to associate this slight red shift with the formation of tartrazine-rich micelles. Because tartrazine generally shows this red shift in less polar solvents such as acetone (λ_{max} = 432 nm),[5] we propose that a polarity decrease in the chromophore microenvironment happens because of the micelle formation. More precisely, as the solution surface is saturated at 0.18 mM, the ion pairs tend to form small premicelles. Further addition of TTAB results in the formation of many more ion pairs and the enlargement of the premicelles so that at 0.49 mM these premicelles are converted to tartrazine-rich micelles. This phase change is reflected by the appearance of a slight surface tension increase (region II of the tensiometry plot) and a red shift. It is reasonable to expect that tartrazine molecules are located in the hydrophilic shell of the micelles because of the intense electrostatic attraction between tartrazine and TTAB molecules as well as because tartrazine interacts solely with the

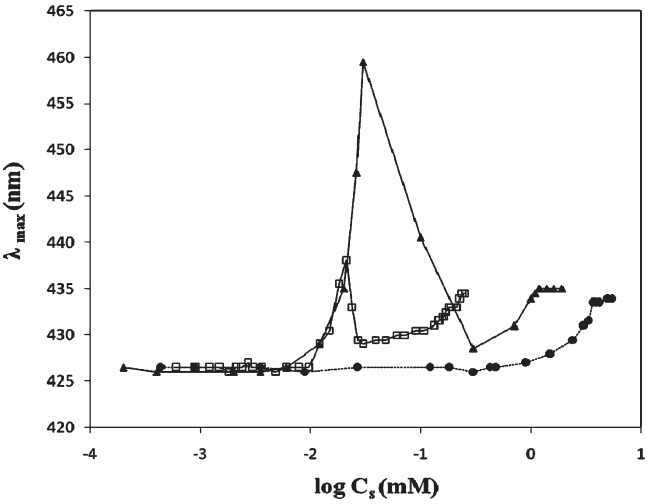

Figure 5. Variation of the maximum absorption wavelength for tartrazine at 426.5 nm with varying concentrations of TTAB (●), 14,4,14 (□), and 12,4,12 (▲).

hydrophilic portion of the surfactant and is completely insoluble in hydrocarbons. Therefore, as the TTAB concentration increases, the aggregation number of tartrazine-rich micelles, and simultaneously, the number of surfactant molecules surrounding the chromophore group of tartrazine increases as well. Dehydration (the replacement of water molecules by surfactants) provides a more nonpolar microenvironment for the chromophore, which gives rise to the observed red shift. The least polar chromophore microenvironment occurs when the highest quantity of surfactant molecules enclose it at the C_2 point where the tartrazine-rich micelles are converted to TTAB-rich micelles. Thus, the λ_{max} is maintained constant at about 435 nm for concentrations above the C_2 point. The solubilization of dye molecules in monomeric form inside the pure surfactant micelles at concentrations above their CMC has already been reported for many systems.[37,38]

In the case of gemini surfactants, a prominent red shift peak also appears soon after the surface saturation. Also, as mentioned above, the solution simultaneously becomes turbid in this concentration range. Aside from these observations, because the tartrazine/TTAB mixture simultaneously lacks both a red shift peak and solution turbidity, the observed red shift peak can be logically accepted to originate from the same species that causes the turbidity in the solution. Such remarkable shifts in the λ_{max} have been attributed to two types of dye aggregates: H-aggregates in which the dye molecules are arranged in the parallel form causing a blue shift, and J-aggregates in which the dye molecules are arranged in the head to tail form causing a red shift.[19,21,39] This transient red shift has been attributed to some size-dependent optical properties of the ion pair-made nanocrystals formed during the aggregation/precipitation/redissolution process.[40] Taking the reported ability of tartrazine to form J-aggregates in the presence of albumin into consideration,[41] the common origin of the observed red shift peak and corresponding turbidity is likely the formation of insoluble J-aggregates through a similar J-aggregation/precipitation/redissolution process. Unlike the single-tail DS^{2-} and/or DS_2^- ion pairs of TTAB, which tend to form small premicelles instead of J-aggregates, the more hydrophobic gemini DS^- ion pairs assemble under the drastic influence of their hydrophobic interactions to

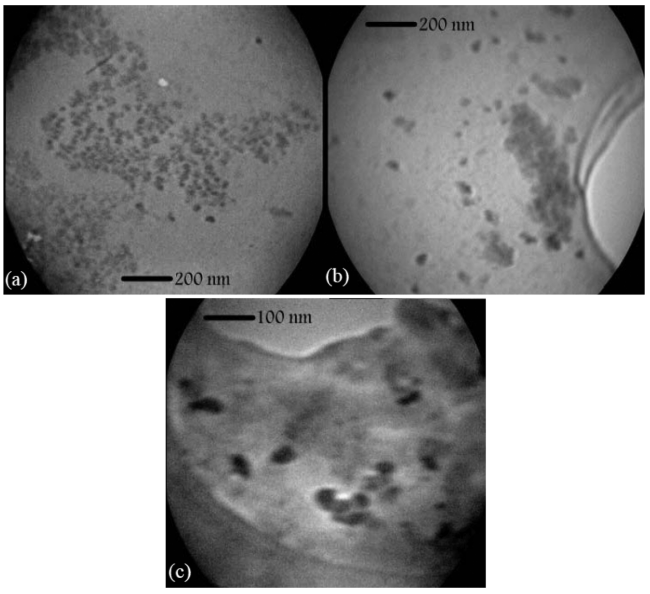

Figure 6. TEM images for tartrazine/12,4,12 system: (a) J-aggregate precipitates (0.02 mM tartrazine + 0.02 mM 12,4,12), (b) preliminary association of J-aggregates to form crystals (0.02 mM tartrazine + 0.02 mM 12,4,12), and (c) cylindrical and ellipsoidal micelles (0.02 mM tartrazine + 2 mM 12,4,12).

form tartrazine J-aggregates. These charged, highly insoluble and amorphous J-aggregates are suspended for several days and then further aggregated to form large yellow crystals that can be seen in TEM images (Figure 6a,b). In the presence of a higher concentration of gemini surfactant, the J-aggregates are converted into soluble tartrazine-rich micelles so that the red shift and the turbidity disappear. Again, the larger peak area for the tartrazine/12,4,12 system compared to that of the tartrazine/14,4,14 system comes from the higher concentration of formed ion pairs and resultant J-aggregates for the former system, which was corroborated by the tensiometry plots. This J-aggregation/precipitation/redissolution process is also reflected in the conductometry plots as a clear break point for both gemini surfactants (12,4,12 and 14,4,14) at approximately 0.025 mM (point A in Figure 7b,c).

Careful examination of Figure 7 reveals that in the presence of tartrazine, the only observed break point for TTAB is the C_2 point and that the conversion of small ion pair premicelles to larger tartrazine-rich micelles cannot be detected by conductometry. Along with the break points at A and C_2 for the geminis, a third break point is observed at a concentration above C_2 (0.24 mM for 14,4,14 and 1.34 mM for 12,4,12). This concentration has been deemed the C_3 point and seems to be related to another micellar phase change from the existing spherical gemini surfactant-rich micelles to the cylindrical micelles. The shape of a micelle is determined by its packing parameter (p) as follows:[36]

$$p = V_H/l_c \times a_0 \quad (6)$$

where V_H is the volume occupied by the hydrophobic portion of the surfactant in the micellar core, l_c is the length of its hydrophobic portion in the core, and a_0 is the cross-sectional area occupied by its hydrophilic portion at the micelle || solution interface. A value of $0 < p < 1/3$ is indicative of the formation of spherical micelles, $1/3 < p < 1/2$ indicates the formation of cylindrical micelles, and lamellar micelles are usually formed at $1/2 < p < 1$. Briefly, the incorporation of tartrazine molecules into the gemini surfactant-rich micelles partially neutralizes their surface charge and facilitates the addition of other surfactant molecules. The aggregation number of the micelles increases, and accordingly, a_0 decreases, resulting in a considerable increase in p and a better packing so that a micellar shape change from spherical to cylindrical may occur. The appearance of some cylindrical and ellipsoidal micelles of 40−70 nm in the TEM image (Figure 6c) confirms the occurrence of such a phase change. A similar phase change from spherical to wormlike micelles has also been reported for cetyltrimethylammonium bromide upon the addition of various aromatic counterions.[42] It is obvious from Table 2 that there is a good accordance between the values of CMC, C_1, C_2, and C_3 obtained by the different techniques.

Taking the above results obtained from conductometry, tensiometry, spectroscopy, and TEM imaging into consideration, the general physicochemical behavior of the studied dye/surfactant systems can now be clarified as follows. First, the primary addition of a small amount of TTAB to the tartrazine solution results in the formation of the nonionic DS_3 ion pairs, which saturate the solution surface. After surface saturation, more hydrophilic DS_2^- and/or DS^{2-} ion pairs and their small premicelles are probably formed. Increasing the TTAB concentration, these small premicelles are converted to tartrazine-rich micelles, which are finally transformed to spherical TTAB-rich micelles with solubilized monomeric dye molecules around the CMC of TTAB. For gemini surfactants, first, the solution surface is saturated by formed DS^- ion pairs. Then, insoluble J-aggregates composed of these ion pairs are formed and eventually converted to soluble tartrazine-rich micelles at higher surfactant concentrations. Through further addition of a gemini surfactant, the existing tartrazine-rich micelles are converted to spherical gemini surfactant-rich micelles with solubilized dye monomers about the CMC point. Finally, another micellar phase change reshapes them into cylindrical micelles at higher concentrations. This entire conversion is also schematically illustrated in Figure 8.

3. 4. Sizes and Zeta Potentials of the Aggregates. Although we also employed the pulsed field gradient NMR (PFG-NMR) technique to obtain the size of the dye/surfactant aggregates in previous work,[43] the application of dynamic light scattering is more useful for this purpose. The former gives only the mean values, but the latter prepares information about size distribution, which is critical to discuss the nature of the aggregates and their probable phase changes happening in the solution. Table 3 lists the obtained sizes and zeta potentials of the aggregates formed in the studied systems. Aggregates with a diameter of 4.12 nm at a 2 mM concentration of TTAB are considered as tartrazine-rich micelles because they are smaller than pure TTAB micelles (4.62 nm). The incorporation of negatively charged tartrazine molecules to the positively charged TTAB hydrophilic shell has decreased the zeta potential (+93 mV → +39 mV). Furthermore, a wide-sized distribution between 1 and 7 nm (peak width = 3.30 nm) implicates the existence of a transformation from small premicelles (1−2 nm) to larger tartrazine-rich micelles, as discussed before. At 5.5 mM, TTAB-rich micelles are formed that have increased diameters (4.93 nm) over the pure TTAB micelles because of the solubilized monomeric tartrazine molecules. This observation corresponds with what we have previously observed for the TTAB/congo red system.[43,44]

For gemini surfactants, along with the tartrazine-rich micelles (3.48 nm diameter for 14,4,14 and 2.68 nm for 12,4,12) and the

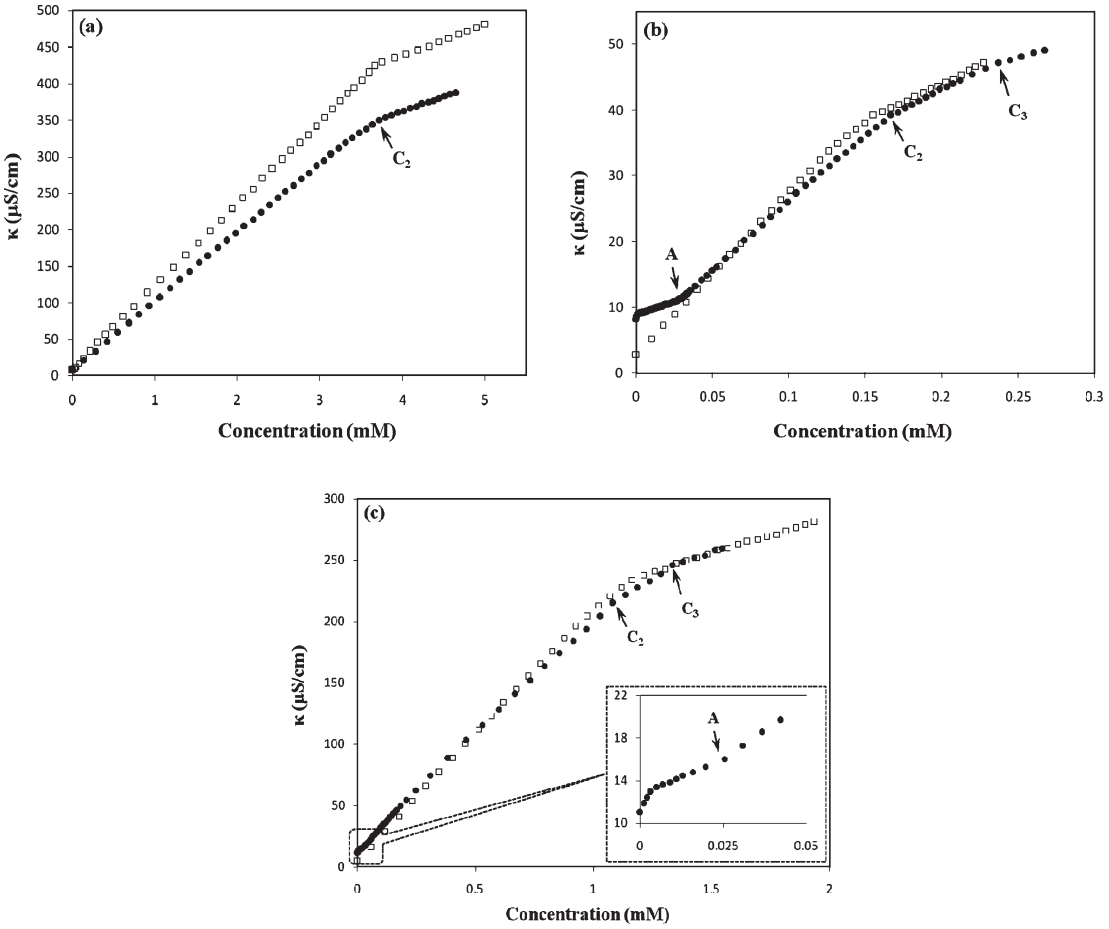

Figure 7. Conductometry plots for (a) TTAB, (b) 14,4,14, and (c) 12,4,12 in the absence of tartrazine (□) and in the presence of 0.02 mM tartrazine (●) at 25 ± 0.1 °C.

Table 2. Values of CMC, C_1, C_2, and C_3 Obtained Using Different Techniques at 25 ± 0.1 °C

			in the presence of 0.02 mM tartrazine			in the presence of 0.02 mM tartrazine + 0.1 M KCl		
surfactant	technique	CMC (mM)	C_1 (mM)	C_2 (mM)	C_3 (mM)	C_1 (mM)	C_2 (mM)	C_3 (mM)
TTAB	conductometry	3.67		3.60				
	tensiometry	3.75	0.18	3.42		0.16	0.88	
	UV−vis			3.61				
14,4,14	conductometry	0.155		0.166	0.24			
	tensiometry	0.152	0.011	0.143		0.0053	0.054	
	UV−vis		0.010	0.18				
	CV					0.0050	0.06	0.10
12,4,12	conductometry	1.12		1.08	1.34			
	tensiometry	1.15	0.0059	1.05		0.0044		
	UV−vis		0.0060	1.20				

spherical gemini surfactant-rich micelles (4.32 nm diameter for 14,4,14 and 3.91 nm for 12,4,12), cylindrical micelles are also formed at concentrations far above the CMCs whose sizes (45.65 nm for 14,4,14 and 60.64 nm for 12,4,12) are in agreement with the TEM image (Figure 6c). The smaller zeta potential values for tartrazine-rich (+8.53 mV) and surfactant-rich (+31.7 mV) micelles of 14,4,14 in comparison to those containing TTAB can be attributed to a larger ratio of tartrazine molecules to micelles. This larger ratio arises from the lower CMC of 14,4,14 and the higher aggregation number of the corresponding micelles, which means that more dye molecules exist at the micelle‖ solution interface. All of the micelles formed in the tartrazine/14,4,14 system are also richer in tartrazine than the 12,4,12 micelles because their zeta potentials are less positive (+8.53 mV → +32.5 mV; +31.7 mV → +50.1 mV; and +93.3 mV → +132 mV). Furthermore, the more positive zeta potential measured for the cylindrical micelles (+93.3 mV for 14,4,14 and +132 mV for 12,4,12) originates from better packing and a

dx.doi.org/10.1021/jp2051323 |J. Phys. Chem. B 2011, 115, 14435–14444

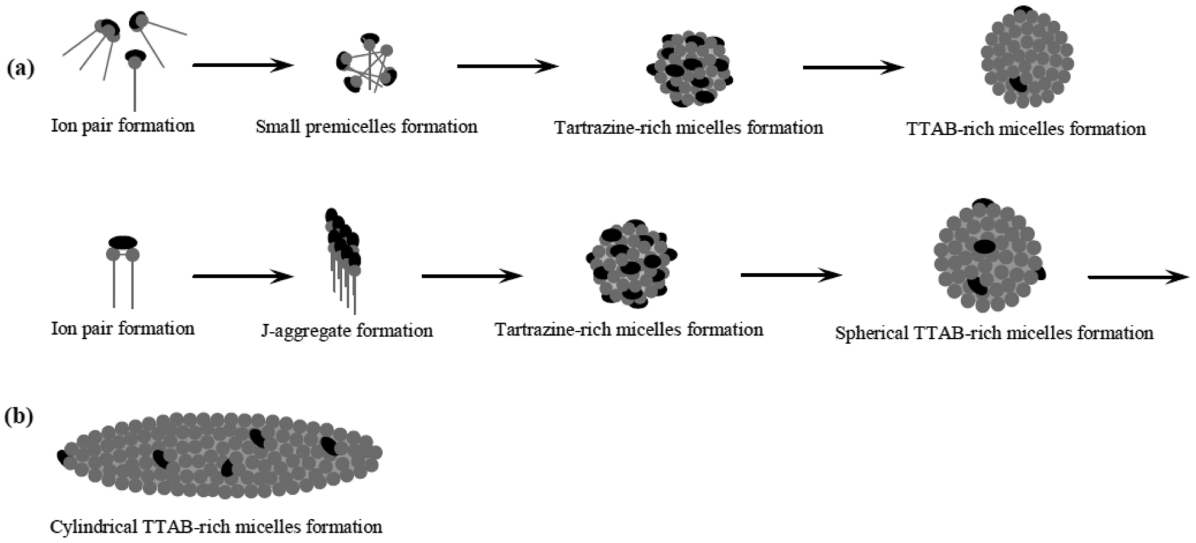

Figure 8. Phase behavior of (a) TTAB and (b) gemini surfactants in the presence of 0.02 mM tartrazine.

Table 3. Hydrodynamic Diameters and Zeta Potentials Obtained for Aggregates at 25 ± 0.1 °C[a]

	TTAB			14,4,14				12,4,12			
parameter	5.5 mM[b]	2 mM[c]	5.5 mM[c]	0.6 mM[b]	0.1 mM[c]	0.2 mM[c]	0.6 mM[c]	1.8 mM[b]	1 mM[c]	1.3 mM[c]	2 mM[c]
diam (nm)	4.62	4.12	4.93	5.48	3.48	4.32	45.65	5.32	2.68	3.91	60.64
	(1.47)	(3.30)	(1.12)	(1.37)	(1.27)	(1.05)	(6.90)	(0.56)	(0.83)	(0.92)	(11.27)
ξ (mV)	+93.4	+39.4	+103	+83.4	+8.53	+31.7	+93.3	+57.2	+32.5	+50.1	+132
	(12.4)	(9.25)	(10.6)	(8.18)	(5.30)	(4.52)	(9.14)	(3.43)	(6.46)	(9.05)	(7.66)

[a] The refraction index and viscosity of the solutions are 1.33 and 0.8872 cP, respectively. Values in parentheses are peak widths at the half-peak height. [b] In the absence of tartrazine. [c] In the presence of 0.02 mM tartrazine.

resulting higher surface charge density. These results once again confirm the suggested model shown in Figure 8.

3. 5. Efficiency of Cyclic Voltammetry in Tracking of Tartrazine/Surfactant Aggregates. There are reports on the direct use of an electroactive probe's peak current to determine the diffusion coefficients and, consequently, the sizes of the aggregates.[45−47] However, this method is not applicable for our system due to the high diversity of the species in the solution, which makes it impossible to determine the exact contribution of each species to the total peak current. Thus, we have to confine ourselves to only tracking the formation of aggregates by following the reduction peak current of tartrazine, which is proportional to the mean diffusion coefficient. For a constant concentration of tartrazine, the formation of any dye-containing aggregate could change the mean diffusion coefficient value and hence the reduction peak current of tartrazine. On the basis of the tensiometry plots and the data listed in Table 2, the electrolyte has no effect on the phase behavior of the studied systems. Only the phase change concentrations (C_1, C_2, and C_3) are reduced, so the results obtained from cyclic voltammetry can be correlated with the behavior of the corresponding tartrazine/surfactant systems in the absence of the electrolyte. The tartrazine/14,4,14 system was chosen to examine the accuracy of this method because the concentrations C_1, C_2, and C_3 are lower and closer together in this system.

Figure 9 shows the variation in the reduction peak current of tartrazine with varying 14,4,14 concentrations, and the resultant voltammograms have been attached as Supporting Information. For the primary concentrations of 14,4,14, the formation and adsorption of heavier DS^- ion pairs decreased the reduction current of tartrazine until the concentration reached 0.0050 mM (point *A*). This point closely matches the concentration (C_1 = 0.0053 mM) at which the ion pairs saturate the solution surface in the presence of an electrolyte (Figure 2b and Table 2). Therefore, the sharp current decrease after point A is related to the J-aggregation/precipitation process that extracts dye molecules from solution on a large scale. Conversely, the redissolution of these J-aggregates in the form of tartrazine-rich micelles causes a sharp current increase starting from point *B* (C_B = 0.02 mM). Because the main parts of the J-aggregates are dissolved, the growth of tartrazine-rich micelles exerts a diminution in the mean diffusion coefficient of tartrazine. Thus, the current starts to decrease again at point *C*. Consequently, the tartrazine-rich to surfactant-rich micelle transformation at point *D* (C_D = 0.06 mM) corresponds well with C_2 = 0.054 mM in the presence of an electrolyte (Table 2). Most of the tartrazine molecules are released again into the solution giving rise to a slight current increase ($\approx 5\,\mu$A), but as the micelles increase in size, the current decreases slowly until another micellar phase change from these spherical micelles to cylindrical micelles occurs at point *E* (C_E = C_3 = 0.1 mM). The formation and growth of the large cylindrical micelles that have solubilized some tartrazine molecules in monomeric form is reflected as the last steep current reduction in the plot.

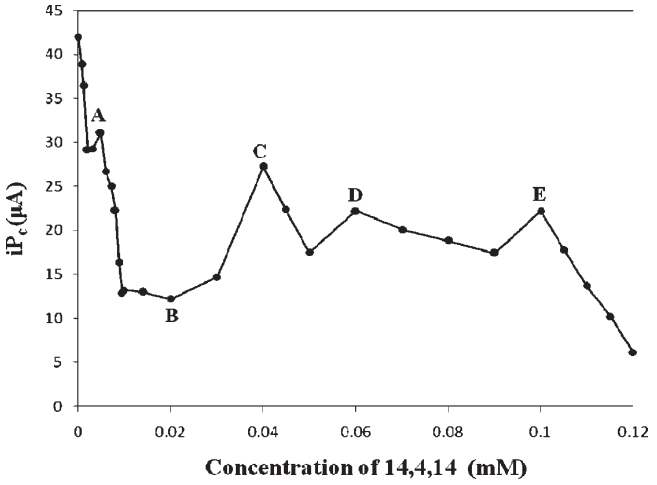

Figure 9. Variation of the cathodic peak current for tartrazine with 14,4,14 concentration. The tartrazine concentration remains constant at 0.02 mM with 0.1 M KCl as a supporting electrolyte. The temperature and scan rate are 25 ± 0.1 °C and 100 mV/s, respectively.

According to these observations, the superb accordance between the results from cyclic voltammetry and the other techniques certifies the competence of cyclic voltammetry in studying dye/surfactant interactions. Moreover, unlike the other methods, which are unable to recognize the existence or formation of some species, cyclic voltammetry can track the formation and the aggregation of ion pairs as well as tartrazine-rich and both spherical and cylindrical surfactant-rich micelles. Thus, although the cyclic voltammetry is not capable of the identification of the nature, shape, and size of the species, it can be highly useful to track all likely phase changes occurring in a dye/surfactant system whose components (one or both) are electroactive themselves.

4. CONCLUSIONS

Unlike most of the organic dyes studied, the function of tartrazine in the presence of surfactants is similar to aromatic counterions. It simply interacts with the polar heads of the surfactants to form ion pairs. Thus, as the surfactant chain length increases, the resulting ion pairs become more hydrophobic and unstable, which result in a decrease in their formation. The surface activity and physicochemical behavior of these ion pairs are heavily dependent on their structure and, in turn, the structure of both the dye and surfactant. Thus, the ion pairs of gemini surfactants are capable of J-aggregation, while those of a conventional surfactant form only dye-rich premicelles and micelles. The partial elimination of long-range electrostatic repulsion originating from the negative charges on tartrazine during ion pair formation is the main cause of this J-aggregation. Simultaneously, the neutralization of the charge on a gemini surfactant exerts a micellar deformation from spherical to cylindrical. The electroactivity of tartrazine makes it possible to track dye-containing species in solution following the reduction peak current by cyclic voltammetry even though the high diversity within the species does not allow for the determination of the diffusion coefficients or the sizes of the aggregates.

■ ASSOCIATED CONTENT

Supporting Information. The visible spectra of tartrazine in the presence and absence of surfactant at various concentrations of dye or surfactant; a plot presenting the linearity of the Beer−Lambert law; and cyclic voltammograms of tartrazine in the presence of 14,4,14. This material is available free of charge via the Internet at http://pubs.acs.org.

■ AUTHOR INFORMATION

Corresponding Author

* Fax: +98-21-82883755. E-mail: javadians@yahoo.com or javadian_s@modares.ac.ir.

■ NOTATION

A_{min}	minimum area per molecule
C_1	concentration of J-aggregation (for gemini surfactants) or ion pair premicelles formation (for TTAB)
C_2	concentration of surfactant-rich micelle formation
C_3	concentration of micellar phase change from sphericals to cylindricals
CMC	critical micelle concentration
ip_c	cathodic peak current
pC_{20}	negative logarithm of the surfactant concentration needed to reduce the solution surface tension by 20 mN/m
Γ_{max}	surface excess concentration
ζ	zeta potential
κ	specific conductivity
λ_{max}	maximum absorption wavelength

■ REFERENCES

(1) Bagha, A. R. T.; Bahrami, H.; Movassagh, B.; Arami, M.; Menger, F. M. *Dyes Pigm.* **2007**, *72*, 331–338.
(2) Yang, J. *J. Colloid Interface Sci.* **2004**, *274*, 237–243.
(3) Scott, G. V. *Anal. Chem.* **1968**, *40*, 768–773.
(4) Pedraza, A.; Sicilia, M. D.; Rubio, S.; Pérez-Bendito, D. *Anal. Chim. Acta* **2004**, *522*, 89–97.
(5) Cruces Blanco, C.; García Campaña, A. M.; Alés Barrero, F. *Talanta* **1996**, *43*, 1019–1027.
(6) Pandit, P.; Basu, S. *Ind. Eng. Chem. Res.* **2004**, *43*, 7861–7864.
(7) Pandit, P.; Basu, S. *Environ. Sci. Technol.* **2004**, *38*, 2435–2442.
(8) Gangotri, K. M.; Meena, R. C.; Meena, R. *J. Photochem. Photobiol., A* **1999**, *123*, 93–97.
(9) Shirota, K.; Kajikawa, K.; Takezoe, H.; Fukuda, A. *Jpn. J. Appl. Phys.* **1990**, *29*, 750–755.
(10) Zoltewicz, J. A.; Munoz, S. *J. Phys. Chem.* **1986**, *90*, 5820–5825.
(11) Akbaş, H.; Kartal, Ç. *Dyes Pigm.* **2007**, *72*, 383–386.
(12) Colichman, E. L. *J. Am. Chem. Soc.* **1950**, *72*, 1834–1835.
(13) Tunç, S.; Duman, O. *Fluid Phase Equilib.* **2007**, *251*, 1–7.
(14) Gohain, B.; Dutta, R. K. *J. Colloid Interface Sci.* **2008**, *323*, 395–402.
(15) Gohain, B.; Boruah, B.; Saikia, P. M.; Dutta, R. K. *J. Phys. Org. Chem.* **2010**, *23*, 211–219.
(16) Gohain, B.; Sarma, S.; Dutta, R. K. *J. Mol. Liq.* **2008**, *142*, 130–135.
(17) Buwalda, R. T.; Jonker, J. M.; Engberts, J. B. F. N. *Langmuir* **1999**, *15*, 1083–1089.
(18) Mukerjee, P.; Mysels, K. J. *J. Am. Chem. Soc.* **1955**, *77*, 2937–2943.
(19) Buwalda, R. T.; Engberts, J. B. F. N. *Langmuir* **2001**, *17*, 1054–1059.

(20) Kapoor, R. C.; Jain, M. K.; Mishra, V. N. *J. Lumin.* **1981**, *22*, 429–439.
(21) Behera, P. K.; Mohapatra, S.; Patel, S.; Mishra, B. K. *J. Photochem. Photobiol., A* **2005**, *169*, 253–260.
(22) Simoncic, B.; Span, J. *Dyes Pigm.* **1998**, *36*, 1–14.
(23) Navarro, A.; Sanz, F. *J. Colloid Interface Sci.* **2001**, *237*, 1–5.
(24) Yousefi, A.; Javadian, S.; Gharibi, H.; Kakemam, J.; Rashidi-Alavijeh, M. *J. Phys. Chem.* **2011**, *115*, 8112–8121.
(25) Mahajan, R. K.; Vohra, K. K.; Shaheen, A.; Aswal, V. K. *J. Colloid Interface Sci.* **2008**, *326*, 89–95.
(26) Jain, R.; Bhargava, M.; Sharma, N. *Ind. Eng. Chem. Res.* **2003**, *42*, 243–247.
(27) Mehedi, N.; Ainad-Tabet, S.; Mokrane, N.; Addou, S.; Zaoui, C.; Kheroua, O.; Saidi, D. *Am. J. Pharmacol. Toxicol.* **2009**, *4*, 128–133.
(28) Wawrzkiewicz, M.; Hubicki, Z. *J. Hazard. Mater.* **2009**, *164*, 502–509.
(29) Craven, B. R.; Datyner, A. *J. Soc. Dyers Colourists* **1963**, *79*, 515–519.
(30) Craven, B.; Datyner, A. *J Soc. Dyers Colourists* **1967**, *83*, 41–43.
(31) El Achouri, M.; Kertit, S.; Gouttaya, H. M.; Nciri, B.; Bensouda, Y.; Perez, L.; Infante, M. R.; Elkacemi, K. *Prog. Org. Coat.* **2001**, *43*, 267–273.
(32) Behera, G. B.; Behera, P. K.; Mishra, B. K. *J. Surf. Sci. Technol.* **2007**, *23*, 1–31.
(33) Navarro, A.; Sanz, F. *Dyes Pigm.* **1999**, *40*, 131–139.
(34) Forte-Tavcer, P. *Dyes Pigm.* **2004**, *63*, 181–189.
(35) Gokturk, S.; Tuncay, M. *J. Surfactants Deterg.* **2003**, *6*, 325–330.
(36) Rosen, M. J. *Surfactants and Interfacial Phenomena*; John Wiley & Sons, Inc.: New York, 2004.
(37) Bielska, M.; Sobczyńska, A.; Prochaska, K. *Dyes Pigm.* **2009**, *80*, 201–205.
(38) García-Río, L.; Hervella, P.; Mejuto, J. C.; Parajó, M. *Chem. Phys.* **2007**, *335*, 164–176.
(39) Chibisov, A. K.; Prokhorenko, V. I.; Görner, H. *Chem. Phys.* **1999**, *250*, 47–60.
(40) Micheau, J. C.; Zakharova, G. V.; Chibisov, A. K. *Phys. Chem. Chem. Phys.* **2004**, *6*, 2420–2425.
(41) de Souza, N. C.; Flores, J. C. J.; Silva, J. R. *Chem. Phys. Lett.* **2009**, *484*, 33–36.
(42) Gamboa, C.; Sepúlveda, L. *J. Colloid Interface Sci.* **1986**, *113*, 566–576.
(43) Rashidi-Alavijeh, M.; Javadian, S.; Gharibi, H.; Moradi, M.; Tehrani-Bagha, A.; Shahir, A. A. *Colloids Surf., A* **2011**, *380*, 119–127.
(44) Shahir, A. A.; Rashidi-Alavijeh, M.; Javadian, S.; Kakemam, J.; Yousefi, A. *Fluid Phase Equilib.* **2011**, *305*, 219–226.
(45) Asakawa, T.; Sunagawa, H.; Miyagishi, S. *Langmuir* **1998**, *14*, 7091–7094.
(46) Ferreira, T. L.; El Seoud, O. A.; Bertotti, M. *J. Electroanal. Chem.* **2007**, *603*, 275–280.
(47) James, J.; Ramalechume, C.; Mandal, A. B. *Chem. Phys. Lett.* **2005**, *405*, 84–89.